

Learning First-Order Rules with Relational Path Contrast for Inductive Relation Reasoning

Yudai Pan, Jun Liu, Lingling Zhang, Xin Hu, Tianzhe Zhao and Qika Lin

Abstract—Relation reasoning in knowledge graphs (KGs) aims at predicting missing relations in incomplete triples, whereas the dominant paradigm is learning the embeddings of relations and entities, which is limited to a transductive setting and has restriction on processing unseen entities in an inductive situation. Previous inductive methods are scalable and consume less resource. They utilize the structure of entities and triples in subgraphs to own inductive ability. However, in order to obtain better reasoning results, the model should acquire entity-independent relational semantics in latent rules and solve the deficient supervision caused by scarcity of rules in subgraphs. To address these issues, we propose a novel graph convolutional network (GCN)-based approach for interpretable inductive reasoning with relational path contrast, named RPC-IR. RPC-IR firstly extracts relational paths between two entities and learns representations of them, and then innovatively introduces a contrastive strategy by constructing positive and negative relational paths. A joint training strategy considering both supervised and contrastive information is also proposed. Comprehensive experiments on three inductive datasets show that RPC-IR achieves outstanding performance comparing with the latest inductive reasoning methods and could explicitly represent logical rules for interpretability.

Index Terms—Knowledge graph, Inductive learning, Rule learning

I. INTRODUCTION

KNOWLEDGE graphs (KGs) store plenty of knowledge by a collection of triples consisting of entities and relations. With the development of KGs including Freebase [1], YAGO [2], DBpedia [3] and Wikipedia [4], the dominant methods have been proposed to learn representations by mapping relations and entities into low-dimension vectors or matrices (i.e. embeddings), such as translation-based models [5, 6], or bilinear models [7, 8]. These methods can be used to predict relations in incomplete triples reasoning.

However, the reasoning task implemented by above methods assumes for a *transductive* setting, which means the entities are fixed during training and testing. According to the open-world assumption, there are new data distributions in the test set meaning unseen entities are waiting for testing, referring to the *inductive* setting. For example, considering the scenario in Fig. 1, entities in the train set and test set have no intersection, so the previous transductive methods will not accurately predict the relation denoted as the blue dotted arrow without retraining

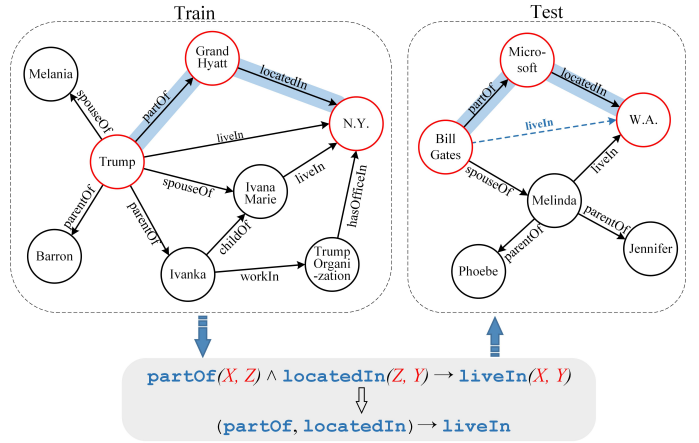


Fig. 1. An example for inductive reasoning.

the whole model. Thus, we focus on models owning inductive ability, which can handle unseen entities in reasoning by mining latent rules during training process, for example,

$$\text{partOf}(X, Z) \wedge \text{locatedIn}(Z, Y) \rightarrow \text{liveIn}(X, Y), \quad (1)$$

where X, Y, Z are variables in the logical rule. The arrow points to the head of Rule (1) and the rest is the body. From Fig. 1, the relation `liveIn` between entities Bill Gates and W.A. in the test subgraph can be inferred by Rule (1) without retraining the model. Existing models of inductive reasoning, for example [9], majorly take advantage of the topological structure of entities and triples in subgraphs, which have an inductive capability and consume less resources. However, there remain two challenges of mining latent rules in inductive reasoning.

Firstly, inductive reasoning has a problem that the test set owns unseen entities during training, which requires entity-independent relational semantics contained in latent rules. The topological structure of entities and triples is difficult to capture semantics of relation sequences in rules which are more critical for entity independence. For example, Rule (1) indicates that entities Trump, Grand Hyatt and N.Y. are generalized to variables X, Y, Z marked in red in Fig. 1, so the entities are less important than connection of relations (`partOf, locatedIn`) for predicting the relation `liveIn` during testing as shown in the gray box.

Secondly, subgraphs own the inductive capability [9], but the scarcity of rules in a single subgraph leads to deficient supervision in inductive learning. Previous statistical methods [10, 11] indicate that in a KG owning m kinds of relations,

Yudai Pan is with the School of Computer Science and Technology, Xi'an Jiaotong University, China e-mail: pyd418@foxmail.com

Jun Liu, Lingling Zhang, Xin Hu, Tianzhe Zhao and Qika Lin are with the School of Computer Science and Technology, Xi'an Jiaotong University

This work has been submitted to the IEEE for possible publication. Copyright may be transferred without notice, after which this version may no longer be accessible.

TABLE I

STATISTICS OF AVERAGE RULES FROM ALL SUBGRAPHS WITH THE MAX RULE LENGTH AS 3 RESPECTIVELY IN A KG. THERE ARE FOUR VERSIONS IN EACH DATASET, WHOSE DETAILS ARE INDICATED IN TABLE IV

Dataset	v1	v2	v3	v4
WN18RR	1.46	1.47	1.43	1.48
FB15K-237	3.13	9.31	16.76	25.27
NELL-995	4.68	15.40	20.95	24.22

the complexity of candidate rules' number within length n is $O(m^n)$, whereas a subgraph only contains a few latent rules. For example in the train subgraph of Fig. 1, there are actually four rules whose length within 3 from entity `Trump` to `N.Y.`, but at least $8^3 = 512$ candidate rules, which is far more than the actual rules. As a note, we treat the reasoning paths as rules like thick blue paths in Fig. 1. More detailed statistics of rules in subgraphs from different datasets are shown in TABLE I. It is unlikely to obtain all the supervised information of candidate rules in a subgraph, which would reduce the performance of the model.

Considering to solve the above challenges, we propose an interpretable approach based on **Relational Path Contrast** for **Inductive Reasoning** named RPC-IR. In order to acquire entity-independent relational semantics, RPC-IR extracts relational paths within a preset length like (`liveIn`, `locatedIn`) in Fig. 1, obtaining representations without variables and entities. To address the deficient supervision of rules in a single subgraph, we propose a contrastive strategy, which is a kind of self-supervised learning methods by constructing positive and negative relational paths. After that, RPC-IR obtains representations of positive and negative relational paths using a graph convolution network (GCN), and proposes a joint training strategy combining the supervised and self-supervised information. In the end, RPC-IR obtains the structure of first-order rules like Rule (1) by relational paths in a single subgraph. The learned rules with confidences can explain the reasoning process in KGs.

Our main contributions can be summarized into three folds:

- An inductive reasoning approach RPC-IR is proposed. We utilize relational paths to represent rules in subgraphs, and design a path representation method to capture the entity-independent information of rules.
- We innovatively devise a contrastive strategy to solve deficient supervision of rules in subgraphs. We firstly employ contrastive learning into inductive reasoning and rule learning tasks.
- Experiments of the relation prediction task on three inductive datasets verify the superiority and effectiveness of RPC-IR. It achieves outstanding performance comparing with latest inductive reasoning methods and explicitly shows the first-order rules for interpretability.

The rest of this paper is organized as follows: Section II surveys previous work about inductive learning in KGs and contrastive learning. Section III comprehensively illustrates the proposed RPC-IR. Section IV demonstrates the effectiveness of RPC-IR by extensive experiments. In section V, we con-

clude the whole paper and put forward the future work.

II. RELATED WORK

We have surveyed the previous related work about inductive learning in KGs and contrastive learning respectively.

A. Inductive Learning in Knowledge Graphs

Inductive learning in KGs requires models own generalization for handling the unseen nodes, which could be divided into two aspects: rule-based and graph-based.

1) *Rule-based*: Previous rule-based methods induce inherent rules from KGs according to statistical patterns. AMIE [11], RuleN [12], AnyBURL [10] and RLvLR [13] mine entity-independent rules by enumerating all the candidates and select rules by preset thresholds. However, these statistical methods are limited to the time complexity and scalability. Different with these, some models are proposed to induce rules in a differentiable pattern, which means to train the model and learn rules by gradient descent in KGs. Yang et al. [14] firstly proposed a differentiable model Neural-LP to learn rules, obtaining the structure and confidence of rules simultaneously by a neural controller system. Sadeghian et al. [15] utilized the bidirectional recurrent neural network (RNN) to capture the backward and forward information about the order of atoms in rules and learn rules with variable lengths. Wang et al.[16] proposed Neural-Num-LP to extend Neural-LP by learning numerical rules and Qu [17] extended Neural-LP by an EM-based algorithm to learn high-quality rules. The above differentiable methods are based on a framework named TensorLog [18] to represent the triples using matrices, whose dimension is the number of entities, so the space complexity would be high. From the descriptions of previous work, rule-based inductive methods in statistical and differentiable pattern will cost enormous time and space resources respectively.

2) *Graph-based*: To solve the scalability and complexity issue, some graph-based methods are proposed for the inductive setting by extracting subgraphs. Teru et al. [9] proposed GraIL to extract subgraphs from KGs and implement the inductive learning by a graph neural network (GNN) with an edge attention mechanism. Mai et al. [19] proposed CoMPLE to strengthen the message interactions between edges and entities through a communicative kernel, and enable a sufficient flow of relation information. Compared with rule-based inductive methods, graph-based inductive methods are more scalable. Distinguished with the above methods, RPC-IR not only utilizes the graph structure, but also captures the entity-independent information by relational paths and solve the deficient supervision of latent rules in subgraphs. In addition, it obtains interpretability in KG reasoning.

B. Contrastive Learning

Contrastive learning, which is a framework of self-supervised learning, consists of methods that obtain representations by learning to encode samples similar or different. Contrastive learning is utilized in the natural language, computer vision and graph domains. As a work in the natural language

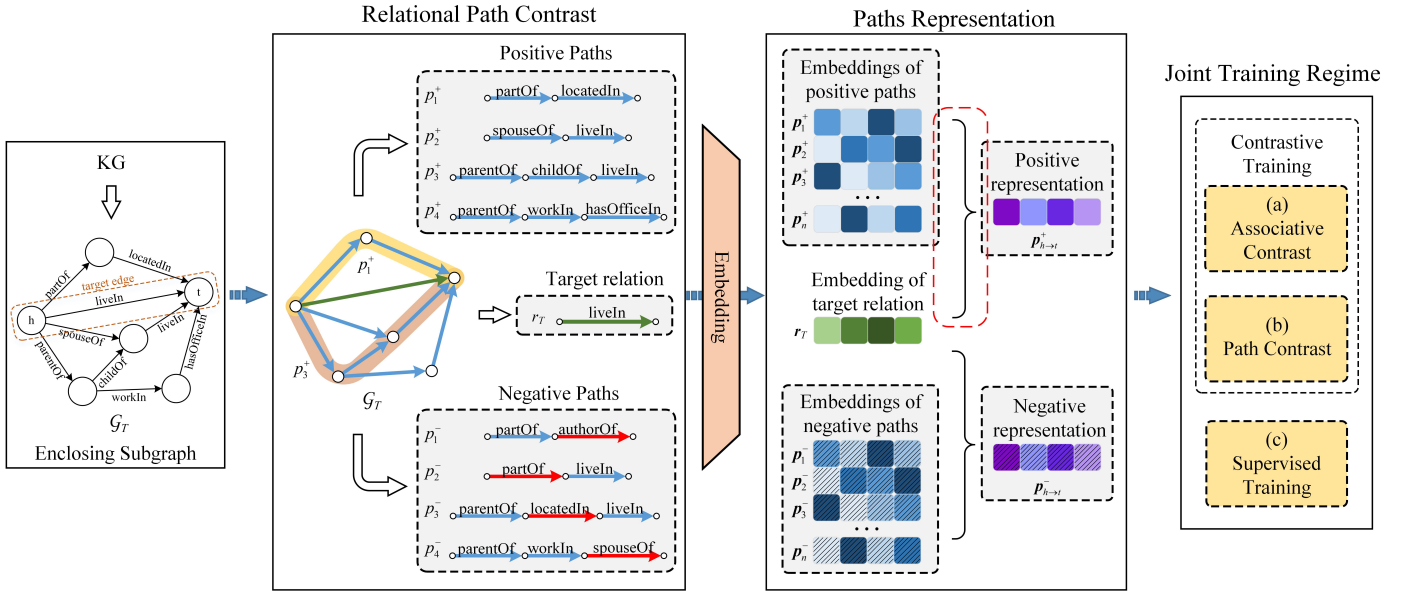


Fig. 2. The framework our RPC-IR.

domain, Oord et al. proposed a contrastive method named CPC [20] to get context latent representations by predicting future information, using a probabilistic contrastive loss. In the field of computer vision, He et al. [21] proposed a contrastive learning framework MoCo for visual representation, which builds large and consistent dictionaries for unsupervised learning with a momentum contrastive loss. Another contrastive method for visual representation is SimCLR [22], which declares that the composition of data augmentation is crucial for contrastive tasks, and illustrates that contrastive learning benefits from larger sizes and more training epochs. In the graph domain, Velickovic [23] proposed deep graph infomax to contrast the patch representations and corresponding high-level summary of graphs. Kipf et al. [24] introduced C-SWMs, utilizing a novel object-level contrastive strategy for representation in environments with compositional structure modeled by GNNs.

These methods utilize contrastive learning for representation on text, images and graphs etc., improving the effectiveness on different downstream tasks. For solving the deficient supervision of rules in subgraphs, we innovatively utilize the contrastive strategy into the inductive reasoning task.

III. METHODOLOGY

This section comprehensively illustrates the inductive reasoning task and our proposed approach RPC-IR.

A. Task Definition and Overview of RPC-IR

Inductive relation reasoning in KGs is to make relation prediction on unseen entities. A target triple e_T is known as a triple (h, r_T, t) in the train KG $G \langle R, E \rangle$, in which h and t refer to the head entity and tail entity, and r_T is the target relation. R and E are sets of relations and entities in G . Relation prediction in a fully-inductive setting intends to quantify the score of target triple e_T and predict the relation between two unseen entities h' and t' in a testing KG

$G' \langle R', E' \rangle$, where $R' \subseteq R$ and $E' \cap E = \emptyset$. In our proposed method, the set of relational paths $\mathcal{P}_{h \rightarrow t}$ in the enclosing subgraph of target triple e_T are extracted and used to score e_T . The RPC-IR can be divided into three steps: 1) extracting paths from the enclosing subgraph of the target triple, and producing positive and negative samples of relational paths for contrast; 2) obtaining representations of positive and negative samples using a GCN; 3) scoring the target triple with the subgraph and relational paths, and training the model by a joint training strategy. After these steps, learned rules are attained by relational paths with their confidences. The demonstration of three steps are shown in the following subsections with the help of Fig. 2.

B. Initialization and Contrast Construction

Firstly in this step, we extract subgraphs from G and obtain features of nodes. Then we generate contrastive samples by constructing positive and negative relational paths. The details are as follows.

Node Features. We extract the enclosing subgraph \mathcal{G}_T based on the target triple e_T from G , and implement the double radius vertex labeling scheme to entities in the subgraph. The node i around target triple (h, r_T, t) is in the intersection of k -hop undirected neighborhoods of h and t . Following [25], the node is labeled as $(d(i, h), d(i, t))$, in which d is the shortest topological distance between two entities. The label of node i is denoted as $[\text{one-hot}(d(i, h)); \text{one-hot}(d(i, t))] \in \mathbb{R}^{(2k+2)}$ to indicate the node feature, where $[\cdot; \cdot]$ refers to the concatenation operation.

Contrastive Relational Paths Generation. After that, relational paths need extracting from the subgraph. In order to select all the topological relational paths of subgraph \mathcal{G}_T , we use breadth first search (BFS) algorithm for extracting every path whose length is no longer than L_{max} from h to t . The set of extracted paths is denoted as $\mathcal{P}_{h \rightarrow t}$. For instance in

Fig. 2, if L_{max} is set as 3, then the algorithm would select 4 relational paths from the extracted subgraph \mathcal{G}_T . Moreover, we design a strategy to generate contrastive relational paths in \mathcal{G}_T by constructing positive and negative samples. We consider the target relation r_T as the original instance and extracted relational paths as the positive path samples. As for the negative samples, they are constructed to distinguish semantics with the original instance and positive samples, so we randomly replace a part of every relational path, and avoid it appearing in the set of positive samples. For example, if the extracted path is (partOf, locatedIn), the negative path would be (partOf, authorOf), in which the replaced relation is denoted as the red arrow in Fig. 2. In following descriptions, the original relation in the subgraph is denoted as r_T , the i -th positive and negative path samples are denoted as p_i^+ and p_i^- respectively. The sets of positive and negative paths are correspondingly indicated as $\mathcal{P}_{h \rightarrow t}^+$ and $\mathcal{P}_{h \rightarrow t}^-$.

C. Paths Representation

The second step of RPC-IR is to get representations of relational paths in the subgraph \mathcal{G}_T . We obtain embeddings of entities and relations using a GCN, and design a strategy for paths representation. The details are in the following.

Subgraph Embedding. We implement a GCN [26] for obtaining embeddings of entities and relations in the KG. The propagation process for calculating the forward-pass update is defined as:

$$z_i^{(k+1)} = \text{ReLU}\left(\sum_{r \in R} \sum_{j \in \mathcal{N}_i^r} \alpha_{i,r} \mathbf{W}_r^{(k)} z_j^{(k)} + \mathbf{W}_{self}^{(k)} z_i^{(k)}\right), \quad (2)$$

where $z_i^{(k+1)}$ denotes the embedding of node i in the $(k+1)$ -th layer. \mathcal{N}_i^r denotes the set of neighbors of entity i connected by relation r . $\mathbf{W}_r^{(k)}$ and $\mathbf{W}_{self}^{(k)}$ refer to the transformation matrices for propagating messages from layer k to $k+1$. $\alpha_{i,r}$ is the edge attention weight corresponding to the edge connected via r , which is obtained following [9]:

$$\mathbf{y}_{i,r} = \sigma_1(\mathbf{W}_1[z_i^{(k)}; z_j^{(k)}; \mathbf{r}; \mathbf{r}_T] + \mathbf{b}_1), \quad (3)$$

$$\alpha_{i,r} = \sigma_2(\mathbf{W}_2 \mathbf{y}_{i,r} + \mathbf{b}_2). \quad (4)$$

\mathbf{r} and \mathbf{r}_T indicate the embeddings of relation r and target relation r_T respectively. σ_1 and σ_2 are activation functions, such as ReLU(\cdot) or Sigmoid(\cdot).

Paths Representation. We design a strategy to obtain representations of relational paths in the subgraph \mathcal{G}_T , which is shown in the red dotted block of Fig. 2 and Fig. 3. In the paths representation step, we use the embeddings of the enclosing subgraph \mathcal{G}_T with entities and relations in it.

Inspired by a rule mining work [7], the relational paths are used to represent the inference process by rules. We calculate the semantic similarity between the target relation r_T and the relational path $p_i \in \mathcal{P}_{h \rightarrow t}$, for r_T and p_i connect the same h and t . Then, we utilize an aggregation function ψ to obtain the representation:

$$\mathbf{p}_{h \rightarrow t} = \psi(\{p_i : p_i \in \mathcal{P}_{h \rightarrow t}\}). \quad (5)$$

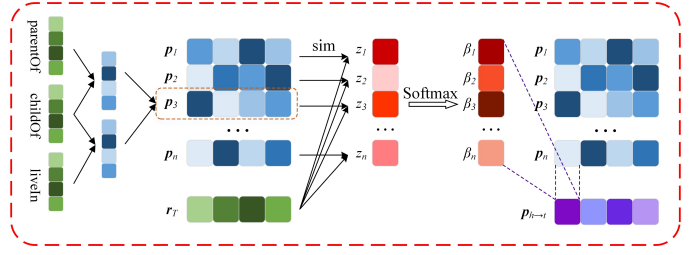


Fig. 3. The process for paths representation.

As illustrated in Fig. 3, p_1, p_2, \dots, p_n are n paths in \mathcal{G}_T , then the representation of the paths is given by:

$$\mathbf{p}_{h \rightarrow t} = \sum_{i=1}^n \beta_i \mathbf{p}_i \quad (6)$$

in which β_i is the attention weight between the path p_i and r_T . \mathbf{p}_i is the representation of path p_i , and we add representations of relations that constructing p_i to represent \mathbf{p}_i , which is implemented by the continuous bag-of-words (CBOW) algorithm. For an alternate strategy, the path representation can be indicated as:

$$\mathbf{p}_i = \sum_{j=1}^{l_i-1} (\mathbf{W}_j r_j^{in} + \mathbf{b}_j), \quad (7)$$

which utilizes a convolution neural network (CNN) to aggregate the relational path, considering the relation sequence. l_i is the number of relations in p_i , and r_j^{in} refers to the j -th window of the relation sequence. For the special condition when $l_i = 1$, we set the representation of the only relation to be \mathbf{p}_i . \mathbf{W}_j is the convolution kernel and \mathbf{b}_j is the optional bias. The attention weight β_i can be regarded as the confidence of corresponding rule for inference in G , which comes from the value of semantic similarity:

$$\beta_i = \text{softmax}(\mathbf{p}_i, \mathbf{r}_T) = \frac{\exp(\mathbf{p}_i^\top \mathbf{r}_T)}{\sum_{p_k \in \mathcal{P}_{h \rightarrow t}} \exp(\mathbf{p}_k^\top \mathbf{r}_T)}, \quad (8)$$

in which p_k refers to each single relational path in $\mathcal{P}_{h \rightarrow t}$. For further contrastive learning, representations of original sample, positive and negative path are \mathbf{r}_T , $\mathbf{p}_{h \rightarrow t}^+$ and $\mathbf{p}_{h \rightarrow t}^-$ respectively, in which $\mathbf{p}_{h \rightarrow t}^+$ and $\mathbf{p}_{h \rightarrow t}^-$ can be acquired with representations of p_i^+ and p_i^- .

Rules and Interpretability. RPC-IR extracts relational paths to capture the entity-independent information during the reasoning process, which can be treated as first-order rules in KGs. After training, RPC-IR obtains relational paths with attention weights, that are actually rules with confidence values extracted from the KG. For example, considering the target relation r_T , if the calculated attention weight of the relational path (r_1, r_2, \dots, r_n) is β , then the structure and confidence $\beta \in [0, 1]$ of the rule are derived simultaneously:

$$\beta r_T(X, Y) \leftarrow r_1(X, Z_1) \wedge r_2(Z_1, Z_2) \wedge r_n(Z_{n-1}, Y). \quad (9)$$

During inference, variables $X, Z_1, Z_2, \dots, Z_n, Y$ are instantiated to entities $x, z_1, z_2, \dots, z_n, y$, and RPC-IR returns a relation with a confidence value by \cdot . There would be several learned rules in a single subgraph that provide the interpretable process of reasoning in KGs.

D. Joint Training Strategy

In this step, we propose a joint training strategy combining the contrastive and supervised information. The contrastive training consists of the associative contrast and path contrast. The detailed descriptions are as follows:

Associative Contrast. In order to associate the topological structure of \mathcal{G}_T denoted as $s_{h \rightarrow t}$ and semantic information from the representation of paths denoted as $p_{h \rightarrow t}$, we score the likelihood of target triple e_T as:

$$s_{h \rightarrow t} = [z_{\mathcal{G}_T}^{(L)}; z_{e_T}^{(L)}], \quad (10)$$

$$f(e_T, \mathcal{P}_{h \rightarrow t}, r_T) = \mathbf{W}_s [s_{h \rightarrow t}; r_T; p_{h \rightarrow t}], \quad (11)$$

where \mathbf{W}_s is the weight matrix. $z_{e_T}^{(L)}$ is the embedding concatenation of (h, r_T, t) of all the L layers' messages, which can be indicated as $[\bigoplus_{i=1}^L (z_h^{(i)}; z_t^{(i)})]$, where \bigoplus is the concatenation operation. $z_{\mathcal{G}_T}^{(L)}$ refers to the global representation of \mathcal{G}_T , which is given by the average readout:

$$z_{\mathcal{G}_T}^{(L)} = \frac{1}{|\mathcal{V}_T|} \sum_{i \in \mathcal{V}_T} z_i^{(L)}, \quad (12)$$

where \mathcal{V}_T refers to the set of nodes in \mathcal{G}_T . We introduce margin-based loss to distance scores of positive and negative samples by an associative contrast:

$$\mathcal{L}_G = \sum_{e_T \in \mathcal{E}} \max(0, \eta + f(e_T^-, \mathcal{P}_{h \rightarrow t}^-, r_T) - f(e_T^+, \mathcal{P}_{h \rightarrow t}^+, r_T)). \quad (13)$$

e_T^+ and e_T^- refer to the positive and negative triple samples, where e_T^- is the sample that replaces the head or tail of e_T^+ . \mathcal{E} is the set of all triples in G . The associative contrast loss is illustrated in Fig. 4(a).

Path Contrast. If we focus more on the semantic information given by relational paths, the contrastive learning should distinguish the target relation with negative paths and make it close to positive paths. Therefore, following the method of InfoNCE loss in [20] and assuming the samples are evenly distributed, the loss for path contrast is defined as:

$$\mathcal{L}_N = -\log \left[\frac{\exp(p_{h \rightarrow t}^+ \top r_T)}{\exp(p_{h \rightarrow t}^+ \top r_T) + \exp(p_{h \rightarrow t}^- \top r_T)} \right]. \quad (14)$$

which is displayed in Fig. 4(b).

Supervised Training. Except for the contrastive learning, we implement the supervised prediction by computing the semantic similarity. With the representation of positive paths $p_{h \rightarrow t}^+$ in \mathcal{G}_T , the supervised learning intends to compare it with the embedding of target relation r_T . In our training strategy, we apply the cross entropy loss on all relation labels in R to minimize the distance between $p_{h \rightarrow t}^+$ and r_T , and maximize the distances with other relations:

$$\mathcal{L}_C = -\log \left[\frac{\exp(p_{h \rightarrow t}^+ \top r_T)}{\sum_{r \in R} \exp(p_{h \rightarrow t}^+ \top r)} \right]. \quad (15)$$

which is shown in Fig. 4(c).

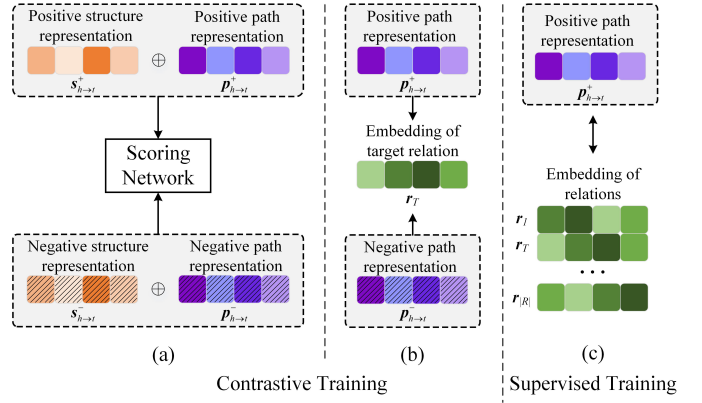


Fig. 4. Joint Training Strategy.

Eventually, the overall loss of our model is defined as the weighted summation of three losses, simultaneously optimizing them by a joint training process:

$$\mathcal{L} = \mathcal{L}_G + \lambda_1 \mathcal{L}_N + \lambda_2 \mathcal{L}_C, \quad (16)$$

where λ_1 and λ_2 are hyperparameters representing weights of path contrast loss and semantic similarity loss.

IV. EXPERIMENTS

In this section, we firstly introduce benchmark datasets, experiment settings and details. Secondly, to verify the effectiveness of RPC-IR, we implement comparison experiments on relation prediction task. In addition, we use ablation studies, hyper-parameter sensitivity analysis and case studies to comprehensively demonstrate the performance.

A. Experimental Settings

Datasets. The inductive link prediction datasets [9] are derived from WN18RR [27], FB15K-237 [28] and NELL-995 [29], and have been generated into four versions respectively. In each dataset, there is no intersection between entities in the train set and test set for the fully-inductive setting. The statistics of benchmark datasets are illustrated in TABLE IV. In particular, each version of a dataset consists of a pair of knowledge graphs, *train* and *ind-test*, whose entities are totally different. Meanwhile, the knowledge graph in *train* contains all the relations in *ind-test*.

Metrics. We demonstrate the effectiveness of RPC-IR by comparing it with other methods on inductive relation prediction tasks. In the comparison, we implement both classification and ranking metrics to evaluate the model.

AUC-PR is an indicator for classification task computing the area under prediction-recall curve. In order to calculate the AUC-PR, we apply the scores considering the subgraph and paths on positive and negative samples.

For the ranking metric Hits@10, we evaluate it in a general mode by ranking the test triples among 50 randomly negative samples. We record the mean results over multiple runs considering the random seeds and samples.

TABLE II

COMPARISON OF AUC-PR (%) RESULTS ON INDUCTIVE BENCHMARKS DERIVED FROM WN18RR, FB15K-237 AND NELL-995. † MEANS WE RERUN THE PROJECT IN THE SAME DEVICE ENVIRONMENT AND RECORD THE RESULTS.

Category	Method	WN18RR				FB15K-237				NELL-995			
		v1	v2	v3	v4	v1	v2	v3	v4	v1	v2	v3	v4
Rule-based	RuleN [12]	90.26	89.01	76.46	85.75	75.24	88.70	91.24	91.79	84.99	88.40	87.20	80.52
	Neural-LP [14]	86.02	83.78	62.90	82.06	69.64	76.55	73.95	75.74	64.66	83.61	87.58	85.69
	DRUM [15]	86.02	84.05	63.20	82.06	69.71	76.44	74.03	76.20	59.86	83.99	89.71	85.94
Graph-based	GraIL [9]	94.32	94.18	85.80	92.72	<u>84.69</u>	<u>90.57</u>	91.68	<u>94.46</u>	<u>86.05</u>	92.62	93.34	<u>87.50</u>
	CoMPILE† [19]	<u>98.29</u>	<u>99.36</u>	<u>93.60</u>	99.51	83.06	90.21	<u>93.12</u>	93.24	82.39	<u>93.30</u>	<u>95.71</u>	52.98
Ours	RPC-IR	98.87	99.41	93.76	<u>98.75</u>	87.24	92.75	93.93	95.26	88.12	94.12	96.10	87.81

TABLE III

COMPARISON OF HITS@10 (%) RESULTS ON INDUCTIVE BENCHMARKS DERIVED FROM WN18RR, FB15K-237 AND NELL-995.

Category	Method	WN18RR				FB15K-237				NELL-995			
		v1	v2	v3	v4	v1	v2	v3	v4	v1	v2	v3	v4
Rule-based	RuleN [12]	80.85	78.23	53.39	71.59	49.76	77.82	87.69	85.60	53.50	81.75	77.26	61.35
	Neural-LP [14]	74.37	68.93	46.18	67.13	52.92	58.94	52.90	55.88	40.78	78.73	82.71	80.58
	DRUM [15]	74.37	68.93	46.18	67.13	52.92	58.73	52.90	55.88	19.42	78.55	82.71	80.58
Graph-based	GraIL [9]	<u>82.45</u>	<u>78.68</u>	58.43	<u>73.41</u>	<u>64.15</u>	81.80	82.83	89.29	<u>59.50</u>	<u>93.25</u>	91.41	<u>73.19</u>
	CoMPILE† [19]	81.91	76.64	<u>60.69</u>	71.80	62.20	<u>82.01</u>	<u>84.67</u>	87.44	58.33	88.86	<u>93.63</u>	60.81
Ours	RPC-IR	85.11	81.63	62.40	76.35	67.56	82.53	84.39	<u>89.22</u>	59.75	93.28	94.01	71.82

TABLE IV
STATISTICS OF DATASETS.

		WN18RR			FB15K-237			NELL-995		
		#R	#E	#Tr	#R	#E	#Tr	#R	#E	#Tr
v1	<i>train</i>	9	2,746	6,678	183	2,000	5,226	14	10,915	5,540
	<i>ind-test</i>	9	922	1,991	146	1,500	2,404	14	225	1,034
v2	<i>train</i>	10	6,954	18,968	203	3,000	12,085	88	2,564	10,109
	<i>ind-test</i>	10	2,923	4,863	176	2,000	5,092	79	4,937	5,521
v3	<i>train</i>	11	12,078	32,150	218	4,000	22,394	142	4,647	20,117
	<i>ind-test</i>	11	5,084	7,470	187	3,000	9,137	122	4,921	9,668
v4	<i>train</i>	9	3,861	9,842	222	5,000	33,916	77	2,092	9,289
	<i>ind-test</i>	9	7,208	15,157	204	3,500	14,554	61	3,294	9,520

Experimental Details. For the subgraph extraction, we obtain 3-hop enclosing subgraphs by the double vertex labeling. In the graph embedding process, we employ a 3-layer GCN with the dimension of the relations and entities as 32. The dropout rate in triples of subgraphs is set to 0.5. When extracting relational paths, we use the max length $L_{max} = 3$ for WN18RR and FB15K-237, and $L_{max} = 2$ for NELL-995 considering the high time complexity. In order to generate negative paths, we randomly replace a relation in each relational path. During the training process, the batch size is set as 16 and we use Adam [30] as optimizer with learning rate being 0.001.

Baselines. The baselines for comparison are previous methods for inductive reasoning in KGs. RuleN [12] is the statistical rule-based inductive method which obtains outstanding performance in the transductive setting. Neural-LP [14] and DRUM [15] are differentiable methods, which generate rules during the reasoning process. Graph-based inductive methods GraIL [9] and CoMPILE [19] can implement inductive rea-

soning as well, but they implement the prediction without interpretability by explicit rules. As a note, to reduce the influence of experimental environment and implement further comparison, we rerun state-of-the-art method CoMPILE [19] with corresponding settings from the original project and record the results. Other results of baselines are from the comparison results in [9].

B. Comparison Results

Comparison of Prediction Results. TABLE II and III show the comparison results of relation prediction. Compared with the listed baselines, RPC-IR significantly outperforms them among the vast majority of datasets in two metrics. The detailed analysis is as follows:

- For the rule-based inductive methods, the average boosts of RPC-IR on WN18RR, FB15K-237 and NELL-995 in AUC-PR are 12.53%, 6.42% and 7.04% respectively compared with the rule-based inductive method RuleN [10]. RPC-IR is also superior to differentiable rule-based inductive methods Neural-LP and DRUM in terms of the classification performance. On the ranking task, RPC-IR outperforms other rule-based inductive methods on most datasets, except for Hits@10 results on FB15K-237_v3 and NELL-995_v4. We attribute this phenomenon to the general performance of graph-based pattern.
- After observation, graph-based inductive methods are generally more effective on most datasets than rule-based inductive methods. Comparing with more competitive graph-based inductive methods, RPC-IR owns optimal results among these datasets in two metrics, which illustrate its superiority as well. RPC-IR results in as much as 6.15%, 2.82% and 2.44% average performance

TABLE V
ABLATION RESULTS OF AUC-PR ON INDUCTIVE BENCHMARKS DERIVED FROM WN18RR, FB15K-237 AND NELL-995.

Method	WN18RR					FB15K-237					NELL-995				
	v1	v2	v3	v4	Avg	v1	v2	v3	v4	Avg	v1	v2	v3	v4	Avg
RPC-IR w/o paths	93.04	95.15	87.48	94.22	92.47	84.56	91.23	91.97	92.90	90.17	81.94	91.59	89.90	73.81	84.31
Δ	$\downarrow 5.83$	$\downarrow 4.26$	$\downarrow 6.28$	$\downarrow 4.53$	$\downarrow 5.23$	$\downarrow 2.68$	$\downarrow 1.52$	$\downarrow 1.96$	$\downarrow 2.36$	$\downarrow 2.13$	$\downarrow 6.18$	$\downarrow 2.53$	$\downarrow 6.20$	$\downarrow 14.00$	$\downarrow 7.23$
RPC-IR w/o contrasts	95.38	95.26	87.90	95.05	93.40	83.71	91.69	93.89	91.85	90.29	82.97	90.83	91.52	78.45	85.94
Δ	$\downarrow 3.49$	$\downarrow 4.15$	$\downarrow 5.86$	$\downarrow 3.70$	$\downarrow 4.30$	$\downarrow 3.53$	$\downarrow 1.06$	$\downarrow 0.04$	$\downarrow 3.41$	$\downarrow 2.01$	$\downarrow 5.15$	$\downarrow 3.29$	$\downarrow 4.58$	$\downarrow 9.36$	$\downarrow 5.60$
RPC-IR	98.97	99.41	93.76	98.75	97.70	87.24	92.75	93.93	95.26	92.30	88.12	94.12	96.10	87.81	91.54

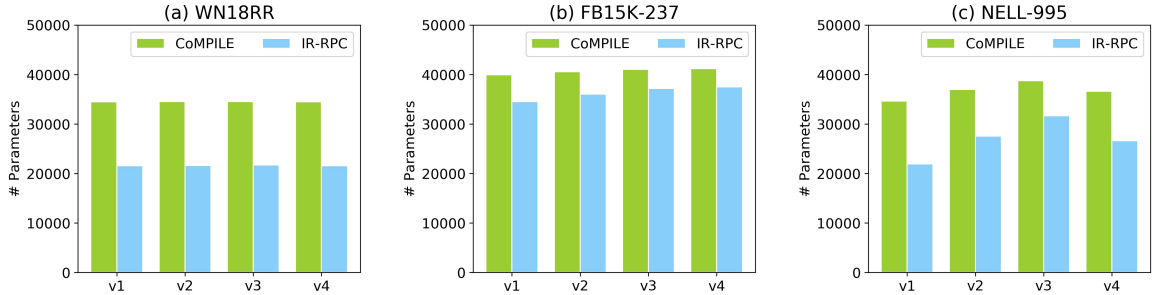


Fig. 5. Comparing numbers of parameters of RPC-IR and state-of-the-art method CoMPILE.

improvements in AUC-PR comparing to GraIL, which is the basic graph-based inductive method. Especially on WN18RR, the classification performance is superior to GraIL, reflecting that the relational path contrast strategy is effective on the more sparse dataset shown in TABLE I. As for the state-of-the-art method CoMPILE, our method performs better on most datasets in terms of both metrics in the same experimental environment.

Comparison of Complexity. Moreover, RPC-IR needs less parameters than the state-of-the-art CoMPILE when training the model, which means we achieve lower model complexity. The results on three datasets are shown in Fig. 5. (a), (b) and (c) severally, in which the green bars refer to the numbers of parameters of CoMPILE, and the blue bars refer to these of RPC-IR. Although RPC-IR owns slightly lower results on a few datasets than CoMPILE, the complexity of RPC-IR is evidently lower than that of CoMPILE on all datasets. For example, CoMPILE gets better AUC-PR value on WN18RR_v4, but owns 34,465 parameters while the number of parameters of RPC-IR is 21,536, reflecting the performance superiority of RPC-IR on WN18RR_v4 from an aspect.

C. Ablation Results

In this subsection, we intend to investigate impacts of relational paths and contrasts in inductive learning respectively. TABLE V indicates the results when training the model by RPC-IR without these factors on all three datasets. For the relational paths, we remove it from our method to verify their contributions and call it “RPC-IR w/o paths”. The same operation is implemented to the contrasts and the method is called “RPC-IR w/o contrasts”. Because of the fair comparison, other parameters remain the same during training and testing.

From TABLE V, we can easily figure that the reduction of AUC-PR values occurs when we train RPC-IR without rela-

tional paths and contrastive learning. After removing relational paths, the average AUC-PR values on WN18RR, FB15K-237 and NELL-995 reduce by 5.43%, 3.00% and 8.01% severally. The lack of contrasts results in corresponding reductions by 4.50%, 2.88% and 6.38% on three datasets. We can also observe that relational paths contribute more in inductive reasoning than contrasts, but better results are obtained by adding relational paths and contrasts simultaneously. In addition, by observing results after removing two factors, it shows that relational paths and contrasts are more effective on NELL-995 than other two datasets.

D. Hyper-parameter Sensitivity Analysis

In this subsection, we analyze the sensitivity of hyper-parameters on different datasets. In our model, λ_1 and λ_2 are critical for adjusting functions of the supervised and self-supervised learning during training, so we rerun the training process in different values of λ_1 and $\lambda_2 \in [0.2, 1.2]$, and record the AUC-PR results to analysis the effectiveness of them. Two versions of datasets, WN18RR_v1 and FB15K-237_v1, are utilized to help achieve the analysis. Considering the training time, we run 150 epochs on WN18RR_v1 and 60 epochs on FB15K-237_v1, and show the test results in of Fig. 5 (a) and (b) respectively. The test results written on the heat maps are mean values after 5 runs.

From the distribution of mean results, we get several observation. Firstly, for WN18RR_v1, better results gather at the lower right corner of the heat map, especially when $\lambda_1 = 1.0$ and $\lambda_2 = 1.2$. Secondly, for FB15K-237_v1, apparently the best results distribute near the diagonal, which means the supervised and self-supervised learning are equally important for inductive reasoning. When $\lambda_1 = 0.8$ and $\lambda_2 = 0.8$, RPC-IR obtains the best test result. The distributions are distinct

TABLE VI
RULES DERIVED FROM THREE VERSIONS OF DATASETS WN18RR_v1, FB15K-237_v1 AND NELL-995_v1.

WN18RR_v1	
0.99	$\text{hypernym}(X, Y) \leftarrow \text{verb_group}(X, Z_1) \wedge \text{hypernym}(Z_1, Z_2) \wedge \text{hypernym}(Z_2, Y)$
0.50	$\text{hypernym}(X, Y) \leftarrow \text{derivationally_related_form}(X, Z_1) \wedge \text{derivationally_related_form}(Z_1, Z_2) \wedge \text{hypernym}(Z_2, Y)$
<0.01	$\text{hypernym}(X, Y) \leftarrow \text{derivationally_related_form}(X, Z) \wedge \text{derivationally_related_form}(Z, Y)$
0.41	$\text{verb_group}(X, Y) \leftarrow \text{derivationally_related_form}(X, Z_1) \wedge \text{derivationally_related_form}(Z_1, Z_2) \wedge \text{verb_group}(Z_2, Y)$
0.41	$\text{verb_group}(X, Y) \leftarrow \text{verb_group}(X, Z_1) \wedge \text{derivationally_related_form}(Z_1, Z_2) \wedge \text{derivationally_related_form}(Z_2, Y)$
0.18	$\text{verb_group}(X, Y) \leftarrow \text{verb_group}(X, Z) \wedge \text{verb_group}(Z, Y)$
<0.01	$\text{verb_group}(X, Y) \leftarrow \text{hypernym}(X, Y)$
FB15K-237_v1	
1.00	$\text{location/contains}(X, Y) \leftarrow \text{location/contains}(X, Z_1) \wedge \text{location/state}(Z_1, Z_2) \wedge \text{location/contains}(Z_2, Y)$
1.00	$\text{location/contains}(X, Y) \leftarrow \text{location/contains}(X, Z) \wedge \text{location/contains}(Z, Y)$
0.45	$\text{location/contains}(X, Y) \leftarrow \text{location/contains}(X, Z) \wedge \text{location/adjoins}(Z, Y)$
<0.01	$\text{location/contains}(X, Y) \leftarrow \text{gardening_hint/split_to}(X, Y)$
0.99	$\text{person/religion}(X, Y) \leftarrow \text{friendship/participant}(X, Z) \wedge \text{person/religion}(Z, Y)$
0.82	$\text{person/religion}(X, Y) \leftarrow \text{dated/participant}(X, Z) \wedge \text{person/religion}(Z, Y)$
<0.01	$\text{person/religion}(X, Y) \leftarrow \text{marriage/type_of_union}(X, Z_1) \wedge \text{location_of_ceremony}(Z_1, Z_2) \wedge \text{location/religion}(Z_2, Y)$
NELL-995_v1	
1.00	$\text{subpartOf}(X, Y) \leftarrow \text{subpartOf}(X, Z) \wedge \text{subpartOf}(Z, Y)$
0.97	$\text{subpartOf}(X, Y) \leftarrow \text{agentBelongsToOrganization}(X, Z_1) \wedge \text{agentBelongsToOrganization}(Z_1, Z_2) \wedge \text{subpartOf}(Z_2, Y)$
0.38	$\text{subpartOf}(X, Y) \leftarrow \text{agentBelongsToOrganization}(X, Z) \wedge \text{subpartOf}(Z, Y)$
<0.01	$\text{subpartOf}(X, Y) \leftarrow \text{agentcollaborateswithagent}(X, Y)$
1.00	$\text{worksFor}(X, Y) \leftarrow \text{agentControls}(X, Z_1) \wedge \text{agentCollaboratesWithAgent}(Z_1, Z_2) \wedge \text{worksFor}(Z_2, Y)$
0.53	$\text{worksFor}(X, Y) \leftarrow \text{worksFor}(X, Z) \wedge \text{subpartOfOrganization}(Z, Y)$
<0.01	$\text{worksfor}(X, Y) \leftarrow \text{topmemberoforganization}(X, Y)$

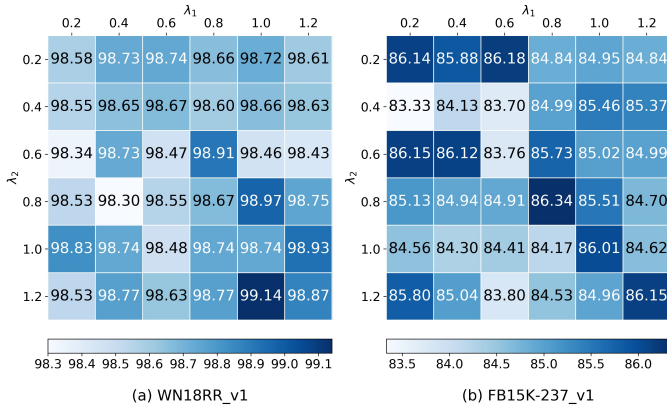


Fig. 6. Effectiveness evaluation by AUC-PR of parameters λ_1 and λ_2 over two datasets.

on different datasets, and it might be related to the number of paths in a subgraph, for the average number paths in an enclosing subgraph of WN18RR are less than that of FB15K-237 shown in Fig. I.

E. Case Studies

As stated in section III, a crucial advantage of RPC-IR in inductive learning is to represent first-order rules for reasoning explicitly. TABLE VI shows examples of derived rules by RPC-IR on the first version of WN18RR, FB15K-237 and NELL-995. The value in front of each rule is the confidence value in the corresponding subgraph. Rules in the same block are with the same head, which is generalized from the target triple, and the body is generalized from the reasoning path when predicting. The rules in red text are with the weight

less than 0.01, which is unreasonable when inference. Overall, RPC-IR implements the interpretability by these explicit rules.

V. CONCLUSION

We propose a novel inductive reasoning and rule learning approach by relational path contrast in KGs, named RPC-IR. To acquire the entity independence semantics from latent rules and solve the deficient supervision in a single subgraph, RPC-IR extracts relational paths in each subgraph and introduces contrastive learning to obtain self-supervised information. The experiments on three fully-inductive datasets show the effectiveness of IR-RPC, and comprehensively demonstrate the impacts for relational paths and contrasts.

RPC-IR still needs improving on scalability and performance. In the future, we intend to implement inductive reasoning and rule learning on more datasets, for example the KGs of curriculum areas, or commonsense knowledge graphs whose entities are free-form texts.

ACKNOWLEDGMENT

The authors would like to thank...

REFERENCES

- [1] K. D. Bollacker, C. Evans, P. Paritosh, T. Sturge, and J. Taylor, "Freebase: a collaboratively created graph database for structuring human knowledge," in *Proceedings of the ACM SIGMOD International Conference on Management of Data, SIGMOD*, 2008, pp. 1247–1250.
- [2] F. M. Suchanek, G. Kasneci, and G. Weikum, "Yago: a core of semantic knowledge," in *Proceedings of the 16th International Conference on World Wide Web, WWW*, 2007, pp. 697–706.

- [3] S. Auer, C. Bizer, G. Kobilarov, J. Lehmann, R. Cyganiak, and Z. G. Ives, “Dbpedia: A nucleus for a web of open data,” in *The Semantic Web, 6th International Semantic Web Conference, 2nd Asian Semantic Web Conference, ISWC*, vol. 4825, 2007, pp. 722–735.
- [4] D. Vrandečić, “Wikidata: a new platform for collaborative data collection,” in *Proceedings of the 21st World Wide Web Conference, WWW*, 2012, pp. 1063–1064.
- [5] A. Bordes, N. Usunier, A. García-Durán, J. Weston, and O. Yakhnenko, “Translating embeddings for modeling multi-relational data,” in *Annual Conference on Neural Information Processing Systems (NIPS)*, 2013, pp. 2787–2795.
- [6] Z. Wang, J. Zhang, J. Feng, and Z. Chen, “Knowledge graph embedding by translating on hyperplanes,” in *Proceedings of the Twenty-Eighth AAAI Conference on Artificial Intelligence*, 2014, pp. 1112–1119.
- [7] B. Yang, W. Yih, X. He, J. Gao, and L. Deng, “Embedding entities and relations for learning and inference in knowledgebases,” in *International Conference on Learning Representations, ICLR*, 2015.
- [8] M. Nickel, V. Tresp, and H. Kriegel, “A three-way model for collective learning on multi-relational data,” in *Proceedings of the 28th International Conference on Machine Learning, ICML*, 2011, pp. 809–816.
- [9] K. K. Teru, E. Denis, and W. Hamilton, “Inductive relation prediction by subgraph reasoning,” in *Proceedings of the 37th International Conference on Machine Learning, ICML*, vol. 119, 2020, pp. 9448–9457.
- [10] C. Meilicke, M. W. Chekol, D. Ruffinelli, and H. Stuckenschmidt, “Anytime bottom-up rule learning for knowledge graph completion,” in *Proceedings of the Twenty-Eighth International Joint Conference on Artificial Intelligence, IJCAI*, 2019, pp. 3137–3143.
- [11] L. A. Galárraga, C. Teflioudi, K. Hose, and F. M. Suchanek, “AMIE: association rule mining under incomplete evidence in ontological knowledge bases,” in *22nd International World Wide Web Conference, WWW*, 2013, pp. 413–422.
- [12] C. Meilicke, M. Fink, Y. Wang, D. Ruffinelli, R. Gemulla, and H. Stuckenschmidt, “Fine-grained evaluation of rule- and embedding-based systems for knowledge graph completion,” in *17th International Semantic Web Conference (ISWC)*, vol. 11136, 2018, pp. 3–20.
- [13] P. G. Omran, K. Wang, and Z. Wang, “Scalable rule learning via learning representation,” in *Proceedings of the Twenty-Seventh International Joint Conference on Artificial Intelligence, IJCAI*, 2018, pp. 2149–2155.
- [14] F. Yang, Z. Yang, and W. W. Cohen, “Differentiable learning of logical rules for knowledge base reasoning,” in *Annual Conference on Neural Information Processing Systems (NIPS)*, 2017, pp. 2319–2328.
- [15] A. Sadeghian, M. Armandpour, P. Ding, and D. Z. Wang, “DRUM: end-to-end differentiable rule mining on knowledge graphs,” in *Annual Conference on Neural Information Processing Systems (NeurIPS)*, 2019, pp. 15 321–15 331.
- [16] P. Wang, D. Stepanova, C. Domokos, and J. Z. Kolter, “Differentiable learning of numerical rules in knowledge graphs,” in *8th International Conference on Learning Representations, ICLR*, 2020.
- [17] M. Qu, J. Chen, L.-P. Xhonneux, Y. Bengio, and J. Tang, “Rnnlogic: Learning logic rules for reasoning on knowledge graphs,” *arXiv preprint arXiv:2010.04029*, 2020.
- [18] W. W. Cohen, “Tensorlog: A differentiable deductive database,” *arXiv preprint arXiv:1605.06523*, 2016.
- [19] S. Mai, S. Zheng, Y. Yang, and H. Hu, “Communicative message passing for inductive relation reasoning,” in *Association for the Advancement of Artificial Intelligence (AAAI)*, 2021.
- [20] A. van den Oord, Y. Li, and O. Vinyals, “Representation learning with contrastive predictive coding,” *arXiv preprint arXiv:1807.03748*, 2018.
- [21] K. He, H. Fan, Y. Wu, S. Xie, and R. B. Girshick, “Momentum contrast for unsupervised visual representation learning,” in *IEEE/CVF Conference on Computer Vision and Pattern Recognition, CVPR*, 2020, pp. 9726–9735.
- [22] T. Chen, S. Kornblith, M. Norouzi, and G. E. Hinton, “A simple framework for contrastive learning of visual representations,” in *Proceedings of the 37th International Conference on Machine Learning, ICML*, vol. 119, 2020, pp. 1597–1607.
- [23] P. Velickovic, W. Fedus, W. L. Hamilton, P. Liò, Y. Bengio, and R. D. Hjelm, “Deep graph infomax,” in *7th International Conference on Learning Representations, ICLR*, 2019.
- [24] T. N. Kipf, E. van der Pol, and M. Welling, “Contrastive learning of structured world models,” in *8th International Conference on Learning Representations, ICLR*, 2020.
- [25] M. Zhang and Y. Chen, “Link prediction based on graph neural networks,” in *Annual Conference on Neural Information Processing Systems, NeurIPS*, 2018, pp. 5171–5181.
- [26] M. S. Schlichtkrull, T. N. Kipf, P. Bloem, R. van den Berg, I. Titov, and M. Welling, “Modeling relational data with graph convolutional networks,” in *The Semantic Web - 15th International Conference, ESWC*, 2018, pp. 593–607.
- [27] T. Dettmers, P. Minervini, P. Stenetorp, and S. Riedel, “Convolutional 2d knowledge graph embeddings,” in *Proceedings of the Thirty-Second AAAI Conference on Artificial Intelligence*, 2018, pp. 1811–1818.
- [28] K. Toutanova, D. Chen, P. Pantel, H. Poon, P. Choudhury, and M. Gamon, “Representing text for joint embedding of text and knowledge bases,” in *Proceedings of the Conference on Empirical Methods in Natural Language Processing, EMNLP*, 2015, pp. 1499–1509.
- [29] W. Xiong, T. Hoang, and W. Y. Wang, “Deeppath: A reinforcement learning method for knowledge graph reasoning,” in *Proceedings of the 2017 Conference on Empirical Methods in Natural Language Processing, EMNLP*, 2017, pp. 564–573.
- [30] D. P. Kingma and J. Ba, “Adam: A method for stochastic optimization,” in *3rd International Conference on Learning Representations, ICLR*, 2015.